Stability of the density-wave state of a dipolar condensate in a pancake-shaped trap

O. Dutta,[*] R. Kanamoto,[†] and P. Meystre

B2 Institute, Department of Physics and College of Optical Sciences, University of Arizona, Tucson, Arizona 85721, USA

We study a dipolar boson-fermion mixture in a pancake-shaped geometry at absolute zero temperature, generalizing our previous work on the stability of polar condensates and the formation of a density-wave state in cylindrical traps. After examining the dependence of the polar condensate stability on the strength of the fermion-induced interaction, we determine the transition point from a ground-state Gaussian to a hexagonal density-wave state. We use a variational principle to analyze the stability properties of those density-wave state.

I. INTRODUCTION

The recent realization of a Bose-Einstein condensate of chromium atoms [1,2] opens up the study of quantum-degenerate gases that interact via the long-range, anisotropic magnetic dipole interaction. This is an anisotropic and long-range interaction that leads to the appearance of a wealth of new properties past those characteristic of systems with isotropic interactions [3]. In the case of ^{52}Cr s-wave interactions are normally much stronger than the dipolar part, but it has been shown experimentally that by applying a magnetic field the s-wave scattering length can be lowered to values comparable to the Bohr radius [4], so that the dipole interaction dominates the system. In the regime where the dipole-dipole interaction is dominant the condensate is characterized by the existence of a metastable state whose properties depends on the trapping geometry [5–7,9–11], as was experimentally demonstrated in Ref. [8]. A roton feature has also been predicted to exist in these systems for appropriate parameters. There would be considerable interest indeed in accessing the associated roton instability [12–14], as it is characterized by the spontaneous generation of a periodic density modulation in the condensate [15]. Unfortunately that state is unstable against collapse, but we found recently that this difficulty can be circumvented by the addition of a small fraction of noninteracting fermions, resulting in a significant stabilization of the bosonic system in cylindrical traps [16]. The simultaneous trapping of bosonic and fermionic isotopes of chromium [17] also points to interesting directions, with the possibility to observe ground and metastable phases in quantum degenerate polar boson-fermion mixtures.

This paper extends our previous study of dipolar boson-fermion mixtures from cylindrical traps to pancake-shaped geometries, showing that dipolar bosons can be stabilized considerably by increasing the boson-fermion s-wave scattering length, and more importantly the density-wave states of dipolar bosons can be stable for typical, zero-field boson-fermion interaction strengths. Section II describes the induced potential created by fermions on bosons, and Sec. III

discusses the general properties of the energy functional as a function of boson-fermion interaction using a variational Gaussian ansatz. Section IV presents an analysis of the transition point to the density-wave state for various combinations of trap aspect ratios and boson-boson contact interaction strengths. Section V introduces a density-wave ansatz in the form of a series of shifted Gaussians. The stability of these density-wave states is determined by varying the width of each Gaussian to seek minima in the interaction energy for various boson-boson s-wave interaction. We find a condition for the stability of these types of density-modulated states. Finally, Sec. VI is a summary and outlook.

II. FERMION-INDUCED INTERACTION IN POLAR CONDENSATES

We consider a mixture of N_b dipolar bosons of mass m_b and N_f single-component fermions of mass m_f confined in a pancake-shaped trap characterized by a tight harmonic potential of frequency ω_z along the z axis and a softer harmonic potential of frequency $\omega_\perp$ in the transverse direction. A polarizing external electric or magnetic field, is taken to be along the z axis. The dipole-dipole interaction between two bosonic particles separated by a distance r is then

$$V_{\mathrm{dd}}(r) = g_{\mathrm{dd}}\left(1 - \frac{3z^2}{r^2}\right)\frac{1}{r^3}, \tag{1}$$

where g_{dd} is the dipole-dipole interaction strength. In the mean-field approximation for the condensate, the energy functional for the order parameter $\phi(\boldsymbol{r})$ of the dipolar condensate can be expressed as

$$
\begin{aligned}
E = &\int \phi^*(\boldsymbol{r})H_0\phi(\boldsymbol{r})d^3r + \frac{gN_b}{2}\int |\phi(\boldsymbol{r})|^4 d^3r \\
&+ \frac{N_b}{2}\int\int |\phi(\boldsymbol{r})|^2 V_{\mathrm{dd}}(\boldsymbol{r}-\boldsymbol{r}')|\phi(\boldsymbol{r}')|^2 d^3r\, d^3r' + E_{\mathrm{ind}},
\end{aligned}
\tag{2}
$$

where

*Corresponding author. dutta@physics.arizona.edu

[†]Present address: Ochanomizu University, Tokyo 112-8610, Japan.

$$H_0 = -\frac{\hbar^2}{2m_b}\nabla^2 + \frac{m_b\omega_z^2}{2}[\lambda^2(x^2+y^2)+z^2] \qquad (3)$$

is the sum of the kinetic energy and the trapping potential and $\lambda = \omega_\perp/\omega_z$. The second term in the energy functional (2) denotes the contact interaction between bosons, characterized by the strength $g = 4\pi\hbar^2 a_{bb}/m_b$ with a_{bb} being the s-wave scattering length, and the third term describes the nonlocal dipole-dipole interaction between bosons. Finally, the last term E_{ind} accounts for the fermion-induced interaction between bosons, given in linear response theory [18]. We describe the fermions in the local density approximation (LDA), which allows us to calculate the induced interaction, and subsequent bosonic quantities, analytically. The basic idea behind that approximation is to assume the local equilibrium of the free fermions with a position-dependent Fermi momentum $k_f(\mathbf{r})$ at each point. This approximation is justified in the case of trapped boson-fermion systems provided that in addition to the familiar LDA validity condition $N_f^{1/3} \gg 1$ for single-component fermionic systems [19], where N_f is the number of fermions, the bosonic and fermionic components are well mixed (no phase separation) and the characteristic length scale of the fermionic component is larger than the bosonic characteristic lengths. These conditions are discussed in more detail in Appendix A.

We assume a contact boson-fermion interaction of strength $g_{bf} = 2\pi\hbar^2 a_{bf}/m_r$, where a_{bf} is the boson-fermion s-wave scattering length and $m_r = m_b m_f/(m_b+m_f)$ is the reduced mass. The boson-fermion interaction energy has the form $g_{bf}\int n_f(\mathbf{k})n(-\mathbf{k})d^3k$, with $n(\mathbf{k})$ and $n_f(\mathbf{k})$ being the bosonic and fermion densities in the momentum space. The linear response of the fermions to a bosonic density $n(\mathbf{k})$ can be expressed as $n_f(\mathbf{k}) = V_{ind}(\mathbf{k})n(\mathbf{k})$, so that for the effect of the fermions on the bosonic energy functional is

$$E_{ind} = \frac{1}{2}\frac{g_{bf}N_b}{(2\pi)^3}\int V_{ind}(\mathbf{k})n(\mathbf{k})n(-\mathbf{k})d^3k. \qquad (4)$$

The explicit form of the induced potential is

$$V_{ind}(\mathbf{k}) = g_{bf}\chi_f(\mathbf{k}), \qquad (5)$$

where χ_f is the density response function [18]. It is related to the dynamical structure factor $S(\mathbf{k},\omega)$, which is the probability of exciting particle-hole pairs with momentum $\mathbf{k}$ out of the Fermi sea, by $\chi_f(\mathbf{k}) = -2\int_0^\infty d\omega'[S(\mathbf{k},\omega')/\omega']$. For a non-interacting single-component Fermi system we have

$$S(\mathbf{k},\omega) = \sum_{\substack{p < k_f \\ |\mathbf{p}+\mathbf{k}| > k_f}}^{\infty}\delta(\omega - \omega_{pk}^0), \qquad (6)$$

where $p = |\mathbf{p}|$, k_f is the Fermi momentum, the excitation energy is $\omega_{pk}^0 = pk\cos\theta/m_f + k^2/(2m_f)$, and θ is the relative angle between $\mathbf{p}$ and $\mathbf{k}$. This expression assumes that the fermions are locally free, so that there is a local Fermi sphere in momentum space. In this local density approximation, k_f is given by [19]

$$k_f\ell_z = 1.9N_f^{1/6}\lambda^{1/3}\sqrt{\frac{m_f}{m_b}}, \qquad (7)$$

where $\ell_z = \sqrt{\hbar/(m_b\omega_z)}$ is the oscillator length in the z direction.

Following Ref. [16] the induced potential $V_{ind}(\mathbf{k})$ is given by

$$V_{ind}(k) = \begin{cases} g_{bf}\nu\left[-1 + \displaystyle\sum_{n=1}^\infty \left(\frac{k}{2k_f}\right)^{2n}\frac{1}{4n^2-1}\right], & k < 2k_f, \\[12pt] -g_{bf}\nu\displaystyle\sum_{n=1}^\infty\left(\frac{2k_f}{k}\right)^{2n}\frac{1}{4n^2-1}, & k > 2k_f, \end{cases}$$

$$\qquad (8)$$

where $\nu = k_f m_f/(\pi\hbar)^2$ is the three-dimensional fermionic density of states, and $k^2 = k_x^2 + k_y^2 + k_z^2$ is the square of the fermionic momentum. The induced potential is attractive for very low momenta and goes to zero with increasing momenta.

Throughout this paper, we consider the parameters corresponding to a ^{52}Cr–^{53}Cr mixture, and fix the number of fermions to be $N_f = 10^3$ unless otherwise stated. The zero-field bosonic s-wave interaction for ^{52}Cr is taken to be $a_{bb} = 103a_0$, and $a_{bf} = 70a_0$ for the boson-fermion scattering length [20].

III. STABILITY OF THE GAUSSIAN DIPOLAR CONDENSATE

We now proceed to determine the stability of the dipolar condensate, using a variational ansatz in the parameter space of the fermion-induced interaction and dipolar strength. The variational wave function is taken as the Gaussian

$$\phi(\mathbf{r}) = \frac{1}{\sqrt{\pi^{3/2}d^2 d_z}}\exp\left(-\frac{x^2+y^2}{2d^2} - \frac{z^2}{2d_z^2}\right), \qquad (9)$$

with d, d_z being the variational parameters and $\int d^3 r|\phi(\mathbf{r})|^2 = 1$. Substituting this Gaussian ansatz and its Fourier transform into Eqs. (2) and (4) yields the energy E_g of the condensate as

$$\frac{m_b\ell_z^2}{\hbar^2}E_g = \frac{1}{2}\left(\frac{1}{2}+\eta^2\right)\left(\frac{\ell_z}{d_z}\right)^2 + \frac{1}{2}\left(\frac{1}{2}+\frac{\lambda^2}{\eta^2}\right)\left(\frac{d_z}{\ell_z}\right)^2$$
$$+ g_{3d}\left(\frac{\ell_z}{d_z}\right)^3\left[\frac{2}{3}\eta^2 - F(\eta^{-1})\right.$$
$$\left. + \left(\frac{d_z}{\ell_z}\right)^3\{g^< E_1^< + g^> E_1^> + g_{ind}(E_2^< - E_2^> + E_3^<)\}\right], \qquad (10)$$

where $\eta = d_z/d$, and $\tilde{k}_f = k_f\ell_z$. The derivation of algebraic forms of the interaction-energy terms $E_1^<, E_1^>, E_2^<, E_2^>, E_3^<$ and of the function F are straightforward but lengthy, and their derivations are relegated to Appendix B. In Eq. (10) we have also introduced the effective three-dimensional dipole-dipole interaction

$$g_{3d} = \frac{m_b N_b g_{dd}}{\sqrt{2\pi}\hbar^2 \ell_z}.$$

The coefficients $g^<$ and $g^>$ find their origin in the momentum-independent contact interaction, given by the summation of the s-wave boson-boson scattering and the constant terms in the induced interaction (8). They are given explicitly by

$$g^< = \frac{g - g_{bf}^2 \nu}{4\pi g_{dd}},$$

$$g^> = \frac{g}{4\pi g_{dd}}. \qquad (11)$$

Finally

$$g_{ind} = \frac{g_{bf}^2 \nu}{48\pi g_{dd} \tilde{k}_f^2}$$

is due to the nonlocal induced interaction. We remark that the effective contact interaction consists of the boson-boson contact interaction as well as the momentum-independent part of the dipole-dipole interaction and of the induced interaction. From Eqs. (10) and (11) we have that for low momenta

$$g_s = \frac{2}{3} + g^<. \qquad (12)$$

It is known that in boson-fermion mixtures without dipolar interaction, phase separation occurs when g_s becomes negative [22–24]. In this paper, in contrast, we restrict our considerations to the case $g_s > 0$ by changing the boson-boson contact interaction g, so that phase separation does not take place.

The energy functional (10) was minimized with respect to η and d_z/ℓ_z for various parameter values, with our results summarized in Fig. 1. Without the fermion induced interaction, $g_{ind} = 0$, the ground-state energy of the system is not bounded from below, and the strong trapping in z direction creates a local minimum in the energy landscape as a function of d_z and η [Fig. 1(a)]. For finite induced interactions $g_{ind} > 0$, we find in contrast that the energy landscape is characterized by two minima, as shown in Figs. 1(b)–1(d). In Fig. 1(b) the global minimum, which occurs for $(\eta, d_z/\ell_z) \simeq (3,2.3)$, is a Gaussian state with narrow width in the transverse x-y plane. The additional local minimum close to $(\eta, d_z/\ell_z) \simeq (0.2, 1.4)$ is a metastable state.

With increasing boson-fermion interaction g_{ind}, though, the ground-state energy corresponding to the global minimum at $\eta > 1$ approaches that of the local minimum [Fig. 1(c)], and these minima eventually reach equal energies at a critical value of g_{ind}. The new ground state past that point is characterized by the parameters $\eta < 1$ and $d_z \sim \ell_z$ [Fig. 1(d)], that is, it is a wide Gaussian in x-y plane.

Experimentally one may either vary the boson-boson s-wave scattering length while keeping the boson-fermion scattering length constant, or vary g_{bf} with constant s-wave interaction g. In a boson-fermion mixture of chromium isotopes, typically $g_{ind} \sim 10^{-3}$ is small, which corresponds to an
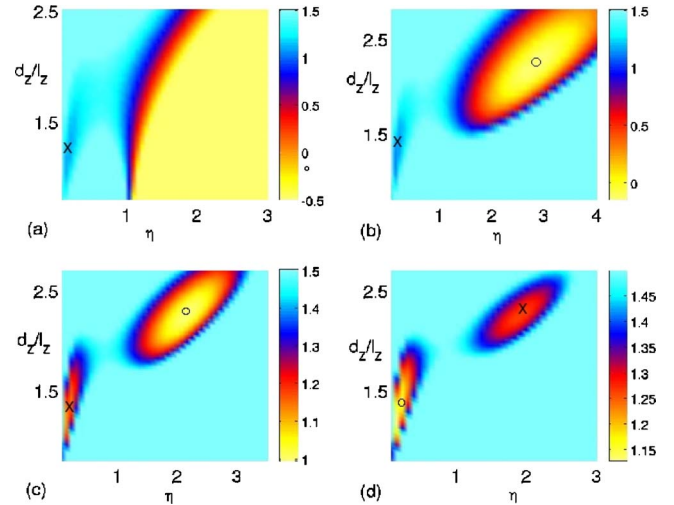

FIG. 1. (Color online) Energy landscape E_g obtained by the variational Gaussian ansatz Eq. (9) as a function of $\eta = d_z/d$ and d_z/ℓ_z at a constant dipolar interaction strength $g_{3d} = 30$. In these figures the energy is cut off at $E_g = 1.5$ from above and $E_g = -0.5$ from below for viewability. (a) Behavior of E_g in the absence of the fermion-induced interaction $g_{ind} = 0$. (b) Energy E_g for $g_{ind} = 0.02$. The plot is characterized by presence of two minima: (i) The true, narrow Gaussian ground state located at $(\eta, d_z/\ell_z) \simeq (3, 2.3)$; and (ii) a pancake-shaped metastable state located at $(\eta, d_z/\ell_z) \simeq (0.2, 1.4)$. (c) Energy landscape for $g_{ind} = 0.06$. The energies of the ground and metastable states approach each other. (d) The broad Gaussian metastable state at $(\eta, d_z/\ell_z) \simeq (0.2, 1.4)$ eventually becomes the true ground state for $g_{ind} = 0.07$. In the figures the global (ground state) and local minima (metastable state) are indicated by a circle and cross, respectively.

energy landscape that resembles that of Fig. 1(b) and the broad Gaussian corresponds to a metastable state. Such a metastable state has been achieved experimentally in experiments by the Stuttgart group [8]. A system that offers the potential to reach the regime of Fig. 1(d) is provided by a mixture of bosonic ^{87}Rb and fermionic ^{40}K with the scattering length of rubidium atoms tuned close to zero. In that mixture, a zero-field scattering length $a_{bf} \approx 250 a_0$ [21] gives $g_{ind} \sim 0.2$.

IV. TRANSITION TO A DENSITY WAVE

The excitation spectrum of condensates dominated by a dipolar interaction is predicted to exhibit a roton minimum [12,13]. As a consequence, a bosonic density-modulated state in the x-y plane may arise as a local minimum, and it may actually have a lower energy than the metastable Gaussian state and for high enough bosonic densities [15]. This section discusses the transition to the appearance of such a state as a function of number of bosonic particles for various combinations of trap ratio.

We proceed by introducing the new variational wave function that describes a density-wave structure with triangular symmetry,

$$\phi_{dw}^t(x,y,z) = \phi(x,y,z)\left\{a_0 + \sum_{n=1}^{\infty} a_n\left[\cos\left(\frac{n\tilde{k}_0 x}{d_z}\right)\right.\right.$$
$$\left.\left. + 2\cos\left(\frac{n\tilde{k}_0 x}{2d_z}\right)\cos\left(n\frac{\sqrt{3}\tilde{k}_0 y}{2d_z}\right)\right]\right\}, \quad (13)$$

where $\phi(x,y,z)$ is defined in Eq. (9), n is an integer, and $\tilde{k}_0 = k_0 d_z \le \eta = d_z/d$. Substituting this trial wave function (13) into Eq. (1), we find that the scaled excess energy of the density-modulated state relative to the Gaussian state

$$\epsilon(\tilde{k}_0, a_1, a_2, a_3) = \frac{2md_z^2}{\hbar^2}(E_{dw} - E_g)$$

is approximately given by

$$\frac{\epsilon(\tilde{k}_0, a_1, a_2, a_3)}{3} \approx \frac{\tilde{k}_0^2}{4}(a_1^2 + 4a_2^2 + 9a_3^2) + \frac{g_{3d}n_d}{4}\left((a_1^2 + 2a_0 a_1\right.$$
$$+ a_1 a_2 + a_2 a_3)^2 V_{eff}(\tilde{k}_0)$$
$$+ (a_1^2 + 2a_1 a_2)^2 V_{eff}(\sqrt{3}\tilde{k}_0)$$
$$+ \frac{1}{4}(a_1^2 + 2a_2^2 + 4a_0 a_2 + 2a_1 a_3)^2 V_{eff}(2\tilde{k}_0)$$
$$+ 2(a_1^2 a_2^2 + a_1^2 a_3^2 + a_2^2 a_3^2)V_{eff}(\sqrt{7}\tilde{k}_0)$$
$$\left. + (2a_0 a_3 + a_3^2)^2 V_{eff}(3\tilde{k}_0)\right), \quad (14)$$

where $n_d \equiv \eta^2 \ell_z/d_z$ [25]. The normalization condition reads as $a_0^2 + 3(a_1^2 + a_2^2 + a_3^2)/2 = 1$, and the effective transverse potential is

$$V_{eff}(\tilde{k}_0) \approx \begin{cases} \frac{2}{3} + g^< - \sqrt{\frac{\pi}{2}}\tilde{k}_0\,\mathrm{erfcx}\left(\frac{\tilde{k}_0}{\sqrt{2}}\right) + g_{ind}\left(\frac{\ell_z}{d_z}\right)^2 \tilde{k}_0^2, & \tilde{k}_0 < 2k_f d_z, \\ \frac{2}{3} + \frac{g}{4\pi g_{dd}} - \sqrt{\frac{\pi}{2}}\tilde{k}_0\,\mathrm{erfcx}\left(\frac{\tilde{k}_0}{\sqrt{2}}\right) - g_{ind}\left(\frac{\ell_z}{d_z}\right)^2 \frac{(2k_f d_z)^4}{\tilde{k}_0^2}, & \tilde{k}_0 > 2k_f d_z. \end{cases} \quad (15)$$

In evaluating Eq. (14) we kept only the first four terms $n = 0,\ldots,3$ of Eq. (13) as the energy converges at the transition point. The magnitude of the error in that approximate expression is estimated to be of the order of $e = \exp(-\tilde{k}_0^2 \eta^2/4)$. In the subsequent calculations we consider values of $\tilde{k}_0$ such that this error is less than or on the order of 10^{-6}.

We numerically determine the variational parameters that minimize the excess energy $\epsilon(\tilde{k}_0, a_1, a_2, a_3)$ as a function of $g^<$ for fixed n_d and g_{3d}. These results are summarized in Fig. 2, which shows the critical number of bosonic particles N_b such that ϵ has a minimum for $\tilde{k}_0 \neq 0$. By tuning the trap aspect ratio $\lambda = \omega_\perp/\omega_z$ to higher values, the critical number of bosons N_b required to achieve $\epsilon < 0$, that is, a transition from a Gaussian to a density-wave metastable state with lower energy, is lowered as a result of an increased n_d. In addition, we note that the value of $\tilde{k}_0$ determined by the present variational calculation matches closely the position of roton minima at the excitation spectrum of the condensate as in Ref. [15]. We also checked the energy with density wave having square symmetry and find that the triangular one always has lower energy.

V. DENSITY WAVE STABILITY

In the preceding section we determined the transition to the density-wave instability, assuming the ansatz (13). As

already mentioned, this transition is related to the existence of a roton minimum in the excitation spectrum. However, assuming such a density wave does not provide an answer to the question of its stability against collapse. This is the issue that we address now, restricting our considerations to the regime where the boson-fermion interaction strength is close to its zero-field value $a_{bf} = 70a_0$. This corresponds in the case
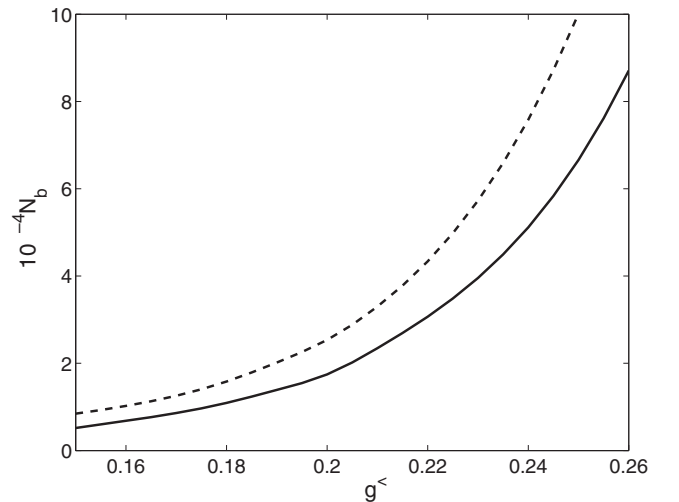

FIG. 2. Critical number of bosonic ^{52}Cr atoms needed for the transition from the Gaussian state to a hexagonal density-wave state for the trap aspect ratios $\lambda = 0.25$ (solid curve) and $\lambda = 0.22$ (dashed curve). Here $\ell_z = 0.15~\mu$m.

of ^{52}Cr-^{53}Cr isotopes to $g_{ind} \sim 10^{-3}$. This is the parameter regime characterized by a Gaussian metastable state, see Sec. II and Fig. 1(b).

Once the transition to the density-wave state has occurred the condensate can also be described as a superposition of shifted Gaussian wave functions within the two-dimensional $Z \equiv x + iy$ plane,

$$\phi_{dw}(Z,z) = \frac{1}{\sqrt{\mathcal{M} \pi^{3/2} \xi^2 d_z}} \sum_{j=1}^{\mathcal{M}} \exp\left(-\frac{(Z-Z_j)^2}{2\xi^2} - \frac{z^2}{2d_z^2}\right),$$

(16)

where j is the index of the lattice site, Z_j the lattice vectors generating periodic density modulations, ξ the width of each density peak, $\mathcal{M}$ the total number of density peaks, and l the distance between neighboring density peaks. It is given by $l = 2\pi/k_0$ where k_0 is the position of roton minimum in the excitation spectrum of the condensate.

Using the results of Sec. III to investigate the stability of each Gaussian in Eq. (16), we now show that the presence of fermions substantially stabilizes the density-wave state, noting that a stable density wave should be characterized by nonzero values of ξ/d_z and d_z/ℓ_z.

From Eq. (16), the total interaction energy is found to be [26]

$$\mathcal{E}_{int}(\xi, d_z) = \frac{m_b \ell_z^2 E_{int}}{\hbar^2} \frac{\mathcal{M}}{g_{3d}}$$

$$= \left(\frac{\ell_z}{d_z}\right)^3 \left[\frac{2}{3}\left(\frac{d_z}{\xi}\right)^2 - F(d_z/\xi) + \left(\frac{d_z}{\ell_z}\right)^3 \{g^< E_1^< + g^> E_1^> + g_{ind}(E_2^< - E_2^> + E_3^<)\} + f(l,\xi,d_z)\right],$$

(17)

where we have assumed that $\xi \ll l$, i.e., that neighboring Gaussian peaks in Eq. (16) have little overlap. Here $E_1^<, E_1^>, E_2^<, E_2^>, E_3^<$ and F have the same form as in the Appendix B, but σ is now a function of (ξ, d_z, θ), $\sigma = \sqrt{d_z^2 \cos^2\theta + \xi^2 \sin^2\theta}$. The function $f(l,\xi,d_z)$ is responsible for the particular geometry of the density-modulated state. Other terms, on the other hand, just arise from the energy of each individual Gaussian and we can thus apply the results of Sec. III to the present analysis.

Assuming a triangular crystal and including only the interaction between nearest neighbors, we have

$$f(l,\xi,d_z) = 6 \int_0^\infty V_{eff}(\tilde{k}) \exp\left(-\frac{\tilde{k}^2 \xi^2}{2d_z^2}\right) J_0\left(\frac{\tilde{k}l}{d_z}\right) \tilde{k} d\tilde{k},$$

with $\tilde{k} = kd_z$, the effective two-dimensional potential $V_{eff}(\tilde{k})$ is defined in Eq. (15), and J_0 is the zeroth-order Bessel function of the first kind.

We now discuss the minimum of the energy functional $\mathcal{E}_{int}(\xi, d_z)$ as a function of the effective strength of the contact interaction g_s, which is varied by changing $g^<$, see Eq. (12). Without boson-fermion interaction, the interaction energy is a monotonically increasing function of ξ with $\mathcal{E}_{int}(\xi \to 0, d_z) \to -\infty$. As a result each Gaussian of the density-wave Equation (16) collapses. A typical example of the dependence of
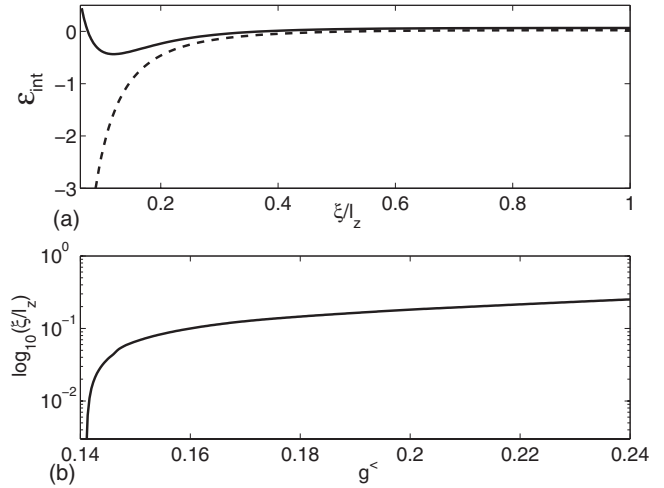

FIG. 3. (a) Interaction energy $\mathcal{E}_{int}$ of Eq. (17) as a function of ξ/ℓ_z at $\lambda = 0.25$, $\ell_z = 0.15$ μm, $d_z = 1.5\ell_z$, and $g^< = 0.18$. For $g_{bf} = 0$ the energy is unbounded from below, but for $g_{bf} = 70a_0$, a minimum appears at $\xi/\ell_z \approx 0.1$. (b) Log-scale plot of the normalized width ξ/ℓ_z that minimizes $\mathcal{E}_{int}$ as a function of $g^<$.

the interaction energy on ξ is shown as the dotted curve in Fig. 3(a). With nonzero boson-fermion interaction energy, in contrast, the interaction energy (17) exhibits a minimum at a finite ξ as illustrated by the solid curve in Fig. 3(a) for $d_z = 1.8\ell_z$ and $g^< = 0.17$. The existence of that minimum implies the stability of each Gaussian, that is, the stability of the wave function (16).

We can determine the dependence of the Gaussian widths ξ on the s-wave boson-boson scattering length by changing $g^<$. To do this we first minimize Eq. (17) as a function of $g^<$, treating d_z and ξ as variational parameters. Figure 3(b) shows the resulting value ξ/ℓ_z as a function of $g^<$ for $\lambda = 0.25$, $N_f = 1000$ and $\ell_z = 0.15$ μm. We observe that ξ decreases for smaller values of the contact interaction $g^<$, and for $g^< \lesssim 0.14$, the minimum-energy state corresponds to the collapsed state, $\xi = 0$. Below that point the density wave is unstable.

This behavior can be understood from the effective potential by first integrating out the z direction to obtain the effective potential $(\ell_z/d_z)^3 V_{eff}(k_\perp d_z)$, where V_{eff} is given by Eq. (15) and $k_\perp^2 = k_x^2 + k_y^2$. The width d_z of the Gaussians is determined by the position of the minimum in Eq. (17). For $g^< \lesssim 0.14$, $V_{eff}(k_\perp d_z)$ is attractive for all high momenta, but at the critical value $g^< \approx 0.14$, it approaches zero as $k_\perp \to \infty$, as shown by the dashed curve in Fig. 4. Hence the energy is always minimized when the wave function has zero width in the x-y plane, i.e., $\xi \to 0$. For $g^< > 0.14$ the effective potential is repulsive both at low and high momenta, and attractive in-between as illustrated by the solid curve in Fig. 4. Subsequently the energy is minimized for a finite value of ξ.

To find the range of parameter space characterized by the appearance of density-wave states, we need to consider, in addition to stability arguments, the transition point discussed in Sec. III. Table I summarizes the range of s-wave scattering lengths and critical numbers of ^{52}Cr atoms necessary to be inside stable density-wave regime.
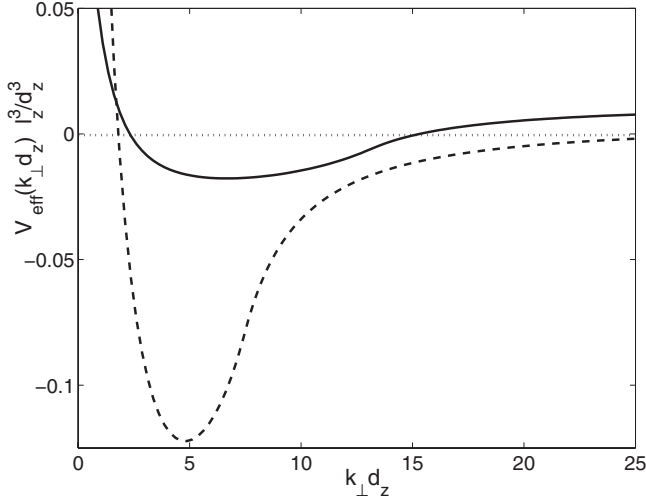
FIG. 4. Effective potential V_{eff} as a function of $k_\perp d_z$ for the parameters of Fig. 3(b) for $g^< = 0.2$ (solid curve), and the critical value of $g^< \approx 0.14$ (dashed curve).

VI. CONCLUSION

In summary, we have analyzed the stability of a dipolar bosonic condensate mixed with noninteracting fermions in a pancake-shaped trap at $T=0$. We found that the fermions help stabilize the condensate for a significant range of boson-boson and boson-fermion interaction strengths. We then investigated the transition of the system from a Gaussian-like to the density-wave ground state as a function of number of bosons, strength of the contact interaction, and trap aspect ratio. Our central result is the use of a variational ansatz to show that while in a purely bosonic system the density-wave state is always unstable it can be stabilized by the admixture of even a small boson-fermion interaction.

In particular, this study leads us to the conclusion that a pancake-shaped ^{87}Rb-^{40}K mixture, which has a large boson-fermion s-wave scattering length, should be absolutely stable in the dipole dominated regime. By tuning the s-wave scattering length it is possible to reach a situation characterized by the appearance of a roton instability in the excitation spectrum, leading to the existence of a stable density-wave state. However, due to the small dipole moment of rubidium atoms the transition to this stable density-wave regime needs a substantial number of atoms, of the order of 10^6.

Future work will discuss the effect of the dipolar nature of the fermionic isotopes on the condensate—with chromium

TABLE I. Tabulation of the scattering length of boson-boson contact interaction a_{bb} and critical number of bosons N_b for different values of aspect ratio λ and oscillator length ℓ_z inside the density-wave regime with $N_f = 10^3$ and $g_{bf} = 70a_0$ for a mixture of chromium isotopes.

λ	ℓ_z (units of μm)	a_{bb} (units of a_0)	$10^{-4}N_b$
0.25	0.15	16–21	$\geqslant 0.65$
	0.2	16–19	$\geqslant 2.3$
	0.25	15–18	$\geqslant 5.0$

atoms in mind—the existence and stability of density waves, as well as possible extensions to rotating systems.

APPENDIX A: VALIDITY OF THE LOCAL DENSITY APPROXIMATION

In deriving the induced interaction Eq. (8) we have introduced a local density approximation (LDA) for fermions in a trapped boson-fermion mixture. For a single component Fermi gas, the LDA is valid as long as the condition [19]

$$k_f(0)R \sim N_f^{1/3} \gg 1 \tag{A1}$$

is satisfied, where $k_f(0)$ is the Fermi momentum at the center of the fermionic density. However, in the case of our boson-fermion mixture two additional conditions need to be satisfied, specifically (i) the bosonic and fermionic components must not be phase separated, and (ii) all characteristic lengths of the bosonic component, such as the Gaussian width of the condensate and the period of the density wave must be less than the characteristic length of the fermions.

To extract these conditions quantitatively, our starting point is the linear-response theory form of the fermion-induced boson-boson interaction energy,

$$E_{\text{ind}} = \int \int V_{\text{ind}}(\boldsymbol{r}, \boldsymbol{r}') n(\boldsymbol{r}) n(\boldsymbol{r}') d\boldsymbol{r} d\boldsymbol{r}' . \tag{A2}$$

Here $V_{\text{ind}}(\boldsymbol{r}, \boldsymbol{r}')$ is the effective boson-boson interaction induced by the fermions.

Transforming into relative and center-of-mass coordinates $\boldsymbol{r} - \boldsymbol{r}'$ and $\boldsymbol{r}_c = (\boldsymbol{r} + \boldsymbol{r}')/2$, taking the Fourier transform with respect to the relative coordinate, and evaluating the integral explicitly for a Gaussian bosonic density profile $n(\boldsymbol{r})$, we obtain the induced-interaction energy for Gaussian condensate

$$\begin{aligned}
E_{\text{ind}} = 2\pi \int & \exp[-2r_c^2(d_z^2\cos^2\theta_c \\
& + d^2\sin^2\theta_c)] r_c^2 dr_c \sin\theta_c d\theta_c \\
& \times \int V_{\text{ind}}(\boldsymbol{r}_c, k) \exp\left(-\frac{k^2}{2}(d_z^2\cos^2\theta \right. \\
& \left. + d^2\sin^2\theta)\right) k^2 dk \sin\theta d\theta .
\end{aligned} \tag{A3}$$

We now invoke the LDA for the fermion component by introducing a position-dependent Fermi momentum $k_f(\boldsymbol{r}_c)$ resulting from the nonuniform fermionic density in the trap. [For an explicit form of the induced interaction we can follow the textbook calculation [18] provided that $k_f \rightarrow k_f(\boldsymbol{r}_c)$.] The induced interaction becomes then

$$V_{\text{ind}}(\mathbf{r}_c, k) = \begin{cases} g_{bf}\nu(r_c)\left[-1 + \sum_{n=1}^{\infty}\left(\dfrac{k}{2k_f(r_c)}\right)^{2n}\dfrac{1}{4n^2-1}\right], & k < 2k_f(r_c), \\[20pt] -g_{bf}\nu(r_c)\sum_{n=1}^{\infty}\left(\dfrac{2k_f(r_c)}{k}\right)^{2n}\dfrac{1}{4n^2-1}, & k > 2k_f(r_c), \end{cases} \tag{A4}$$

where $r_c = |\mathbf{r}_c|$. Evaluating the second integral with respect to $(\mathbf{k}, \theta)$ in Eq. (A3) results in a functional $h[k_f(\mathbf{r}_c)]$ of the Fermi momentum $k_f(\mathbf{r}_c)$,

$$E_{\text{ind}} = 2\pi \int \exp[-2r_c^2(d_z^2\cos^2\theta_c + d^2\sin^2\theta_c)]h[k_f(\mathbf{r}_c)]r_c^2 dr_c \sin\theta_c d\theta_c. \tag{A5}$$

Next we compare the characteristic length scales of bosons and fermions in a trapped system. The mean spatial width of the bosonic Gaussian condensate is $\bar{R}_b = (d^2 d_z)^{1/3}$, and the characteristic length of the fermionic component is given in the LDA by [19]

$$\bar{R}_f \approx \frac{1.9N_f^{1/6}\ell_z}{\lambda^{1/3}}. $$

For the LDA to be valid the fermionic quantities must change slowly in comparison to the bosonic ones, $\bar{R}_f > \bar{R}_b$. If this is satisfied, the Fermi momentum changes slowly in comparison to exponential function in Eq. (A5), and can be replaced by its value at $r_c = 0$,

$$h[k_f(0)] = \int V_{\text{ind}}(k)\exp\left(-\frac{k^2}{2}(d_z^2\cos^2\theta + d^2\sin^2\theta)\right)k^2 dk \sin\theta d\theta,$$

which is the expression used in the main text. In this paper we assume that the number of fermions is of the order of $N_f = 10^3$, so that the condition $\bar{R}_f > \bar{R}_b$ required for the validity of Eq. (10) is

$$\frac{d_z}{\ell_z} < \frac{6.027}{\lambda^{1/3}}\eta^{2/3}. \tag{A6}$$

APPENDIX B: DERIVATION OF THE ENERGY FUNCTIONAL (10)

In this appendix we derive the energy functional Eq. (10) by using the Gaussian ansatz of Eq. (9). First we consider the dipolar interaction energy,

$$E_{\text{dd}} = \frac{g_{\text{dd}}N_b}{3(2\pi)^2}\int d\mathbf{k}\left(3\frac{k_z^2}{k^2} - 1\right)\exp\left(-\frac{1}{2}[k_z^2 d_z^2 + (k_x^2 + k_y^2)d^2]\right), \tag{B1}$$

where $k^2 = k_x^2 + k_y^2 + k_z^2$. Evaluating this integral gives the form of dipolar energy

$$E_{\text{dd}} = \frac{g_{\text{dd}}N_b}{3(2\pi)^2 d_z^3}\left(\frac{2}{3}\eta^2 - F(\eta^{-1})\right), \tag{B2}$$

with $\eta = d_z/d$ and

$$F(y) = \frac{\tan^{-1}(\sqrt{y^2-1})}{(y^2-1)^{3/2}} - \frac{1}{y^2(y^2-1)}.$$

Next we calculate the energy due to s-wave boson-boson interaction and fermion-induced interaction. To achieve this goal we break the integral of the interaction energies expressed in spherical coordinates into two parts, $E_s \equiv E_s^< + E_s^>$ and $E_{\text{dd}} \equiv E_{\text{dd}}^< + E_{\text{dd}}^>$, according to

$$\int_0^{\infty} dk = \int_0^{2k_f} dk + \int_{2k_f}^{\infty} dk. \tag{B3}$$

For $k < 2k_f$ and in spherical coordinate, the interaction energy including the s-wave and induced interaction is given by

$$\begin{aligned} E_s^< &+ E_{\text{ind}}^< \\ &= \frac{g_{\text{dd}}N_b}{2\pi}\int_0^{2k_f}\int_0^{\pi}\left[g^< + \frac{g_{bf}^2\nu}{4\pi g_{\text{dd}}}\sum_{n=1}^{\infty}\left(\frac{k}{2k_f}\right)^{2n}\frac{1}{4n^2-1}\right] \\ &\quad \times \exp\left(-\frac{k^2}{2}(d_z^2\cos^2\theta + d^2\sin^2\theta)\right)k^2 dk \sin\theta d\theta, \end{aligned}$$

where $g^<$ is defined by Eq. (11). This integral contain contribution from both the local and nonlocal part of the induced interaction. After integrating over k and rearranging the terms we obtain the expression

$$E_s^< + E_{\text{ind}}^< = g^< E_1^< + g_{\text{ind}}(E_2^< + E_3^<), \tag{B4}$$

with

$$E_1^<(\sigma) = \int_0^{\pi/2}\frac{\text{erf}(\sqrt{2}k_f\sigma)}{\sigma^3}\sin\theta d\theta,$$

$$E_2^<(\sigma) = \frac{48k_f^3}{\sqrt{2\pi}}\int_0^{\pi/2}\frac{\exp(-2k_f^2\sigma^2)}{\sigma^2}\sin\theta d\theta,$$

$$E_3^<(\sigma) = \frac{3}{\sqrt{2}\pi} \sum_{n=1}^{\infty} \frac{2^{n+1/2}}{4n^2-1} \frac{1}{2k_f^{2(n-1)}}$$

$$\times \int_0^{\pi/2} \left[\frac{\Gamma(n+3/2) - \gamma(n+3/2, 2k_f^2\sigma^2)}{\sigma^{2n+3}} \right] \sin\theta d\theta, \tag{B5}$$

Here $\sigma = \sqrt{d_z^2 \cos^2\theta + d^2 \sin^2\theta}$ is a function of (θ, d_z, d), $\mathrm{erf}(y)$, $\mathrm{erfc}(y)$, Γ, and γ denote the error function, complementary error function, γ function, and incomplete γ function, respectively.

Similarly, the contribution for $k > 2k_f$ to the interaction energy that contains both the s-wave boson-boson interaction and the nonlocal induced interaction is

$$E_s^> + E_{\mathrm{ind}}^> = \frac{g_{\mathrm{dd}}N_n}{2\pi} \int_{2k_f}^{\infty} \int_0^{\pi} \left[g^> - \frac{g_{bf}^2 \nu}{4\pi g_{\mathrm{dd}}} \sum_{n=1}^{\infty} \left(\frac{2k_f}{k} \right)^{2n} \frac{1}{4n^2-1} \right]$$

$$\times \exp\left[-\frac{k^2}{2}(d_z^2 \cos^2\theta + d^2 \sin^2\theta) \right] k^2 dk \sin\theta d\theta,$$

where $g^>$ defined in Eq. (11). In this equation the first term in the bracket stems from the s-wave boson-boson interaction and the last term from attractive nonlocal part of the induced interaction. Again after evaluating the integral over k we obtain

$$E_s^> + E_{\mathrm{dd}}^> = g^> E_1^> - g_{\mathrm{ind}} E_2^> \tag{B6}$$

where

$$E_1^>(\sigma) = \int_0^{\pi/2} \frac{\mathrm{erfc}(\sqrt{2}k_f\sigma)}{\sigma^3} \sin\theta d\theta, \tag{B7}$$

and

$$E_2^>(\sigma) = \frac{3}{\sqrt{2}\pi} \sum_{n=1}^{\infty} \frac{2k_f^{2(n+1)}}{4n^2-1} \int_0^{\pi/2} \left(-\frac{(-1)^n \sqrt{\pi/2}}{(2n-1)!!} \sigma^{2n-3} \right.$$

$$\times \mathrm{erfc}(\sqrt{2}k_f\sigma)$$

$$+ \sum_{m=0}^{n-2} \frac{(-1)^m 2^{m+1}(2k_f)^{2m}}{2k_f^{2n-2m-3}(2n-3)(2n-5)\cdots(2n-2m-3)}$$

$$\times \exp(-2k_f^2\sigma^2)\sigma^{2m} \Bigg) \sin\theta d\theta, \tag{B8}$$

The total interaction energy is the sum of the contributions in Eq. (B2), (B4), and (B6) and is given in Eq. (10). In the present paper we took $n = 1, \ldots, 3$ in the series in Eqs. (B5) and (B8) as the energy E_g in Eq. (10), as they are sufficient to reach an adequate convergence.

[1] A. Griesmaier, J. Werner, S. Hensler, J. Stuhler, and T. Pfau, Phys. Rev. Lett. **94**, 160401 (2005).

[2] Q. Beaufils, R. Chicireanu, T. Zanon, B. Laburthe-Tolra, E. Marechal, L. Vernac, J. C. Keller, and O. Gorceix, Phys. Rev. A **77**, 061601(R) (2008).

[3] K. Góral, L. Santos, and M. Lewenstein, Phys. Rev. Lett. **88**, 170406 (2002).

[4] T. Lahaye, T. Koch, B. Fröhlich, M. Fattori, J. Metz, A. Griesmaier, S. Giovanazzi, and T. Pfau, Nature (London) **448**, 672 (2007).

[5] L. Santos, G. V. Shlyapnikov, P. Zoller, and M. Lewenstein, Phys. Rev. Lett. **85**, 1791 (2000).

[6] S. Yi and L. You, Phys. Rev. A **63**, 053607 (2001).

[7] C. Eberlein, S. Giovanazzi, and D. H. J. O'Dell, Phys. Rev. A **71**, 033618 (2005).

[8] T. Koch, T. Lahaye, J. Metz, B. Fröhlich, A. Griesmaier, and T. Pfau, Nat. Phys. **4**, 218 (2008).

[9] K. Góral, K. Rzażewski, and T. Pfau, Phys. Rev. A **61**, 051601(R) (2000).

[10] S. Ronen, D. C. E. Bortolotti, and J. L. Bohn, Phys. Rev. Lett. **98**, 030406 (2007); S. Ronen, and J. L. Bohn, Phys. Rev. A **76**, 043607 (2007).

[11] O. Dutta and P. Meystre, Phys. Rev. A **75**, 053604 (2007).

[12] L. Santos, G. V. Shlyapnikov, and M. Lewenstein, Phys. Rev. Lett. **90**, 250403 (2003).

[13] U. R. Fischer, Phys. Rev. A **73**, 031602(R) (2006).

[14] S. Komineas and N. R. Cooper, Phys. Rev. A **75**, 023623 (2007).

[15] Y. Pomeau and S. Rica, Phys. Rev. Lett. **72**, 2426 (1994); C. Josserand, Y. Pomeau, and S. Rica, *ibid.* **98**, 195301 (2007), and reference therein.

[16] O. Dutta, R. Kanamoto, and P. Meystre, Phys. Rev. Lett. **99**, 110404 (2007).

[17] R. Chicireanu, A. Pouderous, R. Barbé, B. Laburthe-Tolra, E. Maréchal, L. Vernac, J.-C. Keller, and O. Gorceix, Phys. Rev. A **73**, 053406 (2006).

[18] P. Nozières and D. Pines, *The Theory of Quantum Liquids* (Perseus, Cambridge, 1999).

[19] C. J. Pethick and H. Smith, *Bose-Einstein Condensation in Dilute Gases* (Cambridge University Press, Cambridge, 2002).

[20] Tilman Pfau (private communication).

[21] J. Goldwin, S. Inouye, M. L. Olsen, B. Newman, B. D. DePaola, and D. S. Jin, Phys. Rev. A **70**, 021601(R) (2004), and reference therein.

[22] J. M. J. van Leeuwen and E. G. D. Cohen, Phys. Rev. **176**, 385 (1968).

[23] H. P. Büchler and G. Blatter, Phys. Rev. Lett. **91**, 130404 (2003).

[24] Z. Akdeniz, P. Vignolo, A. Minguzzi, and M. P. Tosi, J. Phys. B **35**, L105 (2002); P. Capuzzi, A. Minguzzi, and M. P. Tosi, Phys. Rev. A **68**, 033605 (2003).

[25] For a fixed number of dipolar bosons, the quantity n_d can be changed by tuning the aspect ratio λ.

[26] The qualitative behavior of the total energy landscape, hence the stability of the density-wave state, remains unchanged by the inclusion of the kinetic energy and trapping potential.